Available online at www.sciencedirect.com
ScienceDirect
Journal of Power Sources 161 (2006) 323–332
JOURNAL OF POWER SOURCES
www.elsevier.com/locate/jpowsour

Effects of the gas diffusion-layer parameters on cell performance of PEM fuel cells

Jer-Huan Jang [a], Wei-Mon Yan [b,*], Chinh-Chang Shih [a]

[a] *Department of Mechanical Engineering, Northern Taiwan Institute of Science and Technology, Pei-To, Taipei 112, Taiwan, ROC*
[b] *Department of Mechatronic Engineering, Huafan University, Shih Ting, Taipei 223, Taiwan, ROC*

Received 17 February 2006; received in revised form 30 March 2006; accepted 30 March 2006
Available online 26 May 2006

Abstract

The characteristic parameters of the gas diffusion-layer (GDL) on cell performance and mass transfer of a proton exchange membrane fuel cell have been investigated numerically. A two-dimensional, isothermal and multi-phase numerical model has been established to investigate the influence of the GDL parameters on the transport phenomenon and cell performance of PEM fuel cells. The porosity and thickness of the GDL are employed in the analysis as the parameters. In addition, the effects of liquid water and the flow direction of the fuel and air on the performance are also considered in this paper. The results show that both the porosity and thickness of the GDL affect the fuel cell performance significantly, especially the water mass transfer. It is shown that the cell performance with consideration of a liquid water effect is always less than that without consideration of the liquid water effect. In addition, the cell performance with a co-flow pattern of fuel and air is better than that with a counter flow pattern.

Keywords: PEM fuel cell; Gas diffuser layer; Porosity; Thickness; Liquid water effect

1. Introduction

The proton exchange membrane fuel cell (PEMFC) is a promising alternative power plant for transportation due high efficiency, low emission, low noise and a low operating temperature [1–4]. The gas diffusion layers (GDLs) of the fuel cell is required to provide both reactant gases to the catalyst layer and removal of water in either vapor or liquid form in a typical PEMFC. Although it seems to be a minor component in a fuel cell, the GDL is one of the most important parts of a PEM fuel cell. A detailed study was done by Moreira et al. [5] on the influence of the hydrophobic material content in the gas diffusion electrode on the performance of the membrane electrode assembly (MEA). Jordan et al. [6,7] experimentally examined the influence of the diffusion-layer morphology on cell performance. They developed a model of the hydrophobilicity and porosity of the diffusion layer to explain the influence of the diffusion-layer morphology and showed that a low-porosity acetylene black enhances water removal from the MEA. Recently, the effects of the fabrication method and the thickness of the GDL on the cell performance were experimentally studied by Lee et al. [8]. However, their study was focused on the fabrication method of the GDL—rolling, spraying and screen printing, in affecting the cell performance.

Because experimental work is costly, numerical modeling becomes an efficient and convenient approach to fuel cell analysis. For the last decade, much effort has been involved in the development of a numerical model with increasingly less restrictive assumptions and more physical complexities. Several examples of analysis of PEM fuel cells can be found in the literature [9–12]. The first 1D model of a PEM fuel cell was developed by Springer et al. [13]. Bernardi and Verbrugge [14] developed a 1D hydraulic model and assumed that the membrane is fully saturated with water and that most of the water is transported through the electrodes in the liquid phase. The first quasi-2D, along-the-channel model of a PEM fuel cell was established by Fuller and Newmann [15] with the assumption of constant diffusivity of water in the membrane. Gurau et al. [16] presented a comprehensive model for the entire sandwich of a PEMFC including the gas channels and considered the gas–liquid phases

* Corresponding author.
E-mail address: wmyan@huafan.hfu.edu.tw (W.-M. Yan).

0378-7753/$ – see front matter © 2006 Elsevier B.V. All rights reserved.
doi:10.1016/j.jpowsour.2006.03.089

Nomenclature

a	chemical activity of water vapor in cathode
Aj_0	exchange current density (A m^{-3})
C	concentration
C_F	quadratic drag factor
D	diffusivity (m^2 s^{-1})
F	Faraday constant, 96485 c mol^{-1}
i	current density (A m^{-2})
j	current density (A m^{-3})
k	permeability (m^2)
M	molecular weight
P	pressure (atm)
P_i	partial pressure for i species (atm)
R	universal gas constant (8.314 J mol^{-1} K^{-1})
s	saturation, the ratio of the volume of pore occupied by liquid water to the volume of pore in the porous medium
S	source term in momentum equation (m s^{-2})
S_c	source term of chemical reaction in the species concentration equation (s^{-1})
S_j	source term in phase potential equation (A m^{-3})
S_L	source term with consideration of liquid water in the species concentration equation (s^{-1})
t	thickness (m)
T	temperature (K)
U, V	velocities in the X and Y direction (m s^{-1})
X, Y	rectangular coordinate system (m)
Z	number of electrons transferred
Z_f	charge transfer coefficient

Greek symbols

α	charge transfer rate
ε	porosity
η	overpotential
ν	kinematic viscosity (m^2 s^{-1})
ρ	density (kg m^{-3})
σ	electric conductivity (1 Ω^{-1} m^{-1})
τ	tortuosity of the pore in the porous medium
Φ	membrane potential

Superscripts and subscripts

a	quantity in anode
c	quantity in cathode
eff	effective value
g	of gas diffuser layer
H^+	for proton
H_2	for hydrogen
H_2O	for water
i	for i species
m	of membrane
O_2	for oxygen
ref	reference value
sat	saturation pressure for water vapor
x	in the X-direction
y	in the Y-direction

in the separate computation domains for transport in the gas distribution channels. Hsing and Futerko [17] developed a 2D model of coupled fluid flow, mass transport and electrochemistry of a PEMFC by taking into account the dependence of the diffusion coefficient of liquid water in the membrane. However, these 2D models do not resolve the catalyst layers and hence ignore the influence of spatial non-uniformity of water content on the catalyst layer performance.

Gurau et al. [18] proposed a 1D mathematical model to obtain an analytic solution of the mass transport of reactant gas in a half-cell, in which the effects of the porosity and the tortuosity of the GDL and the catalyst layer were explored due to the fact that the pores may be partially filled with liquid water. Chu et al. [19] also used a half-cell model to investigate the effects of non-uniform porosity on fuel cell performance in terms of physical parameters such as oxygen consumption, current density and power density, etc. Later, Yan et al. [20] conducted a numerical study with 2D half-cell mass transport model to study the effects of fuel channel width and GDL porosity on the cross-cell transport of reactant gas and the performance of a PEM fuel cell. Recently, Weber and Newman [21] reviewed on the modeling transport in PEM fuel cells to discuss the different fuel-cell models with various types of transport in fuel cells focusing on the transport of the various species within the fuel cell. In this paper, they had made an overview for the numerical modeling work.

To consider the water management of the fuel cell, many of the studies investigated the water transport of the two-phase flow system in which relevant heat transfer problems were also taken into account. Some studies considered the physical domain including the gas diffusion layer, the catalyst layer and the membrane [22–28], while some focused on the membrane [29,30]. A common conclusion from these studies was that the operational current density, the humidification parameter and the membrane thickness had a significant influence on the water transportation in the fuel cell. From the literature review above, it is found that a full-cell mathematical model with consideration of the catalyst layer and membrane water transport in a PEMFC has not been well examined yet. This motivates the present study. The objective of this work is to establish a 2D, full-cell mathematical model with consideration of water saturation, in order to investigate the effects of both the porosity and size scale of gas diffuser-layer on the cell performance of PEMFCs. Additionally, the effect of flow directions of fuel and air on the cell performance is also taken into account in the analysis.

2. Analysis

The PEM fuel cell model described in this study is developed to analyze the characteristics of the GDL. The computational domain is the full cell, which includes a membrane sandwiched between two gas diffusion electrodes, and the flow channels of both the anode and cathode. Fig. 1 shows a schematic illustration of a PEMFC in the co-flow mode with the coordinate system. The U and V are the velocity components in the X- and Y-directions, respectively. The PEMFC in the counter-flow mode is also examined to study the performance of a PEMFC between the co-flow and the counter-flow modes for comparison. Consequently, to

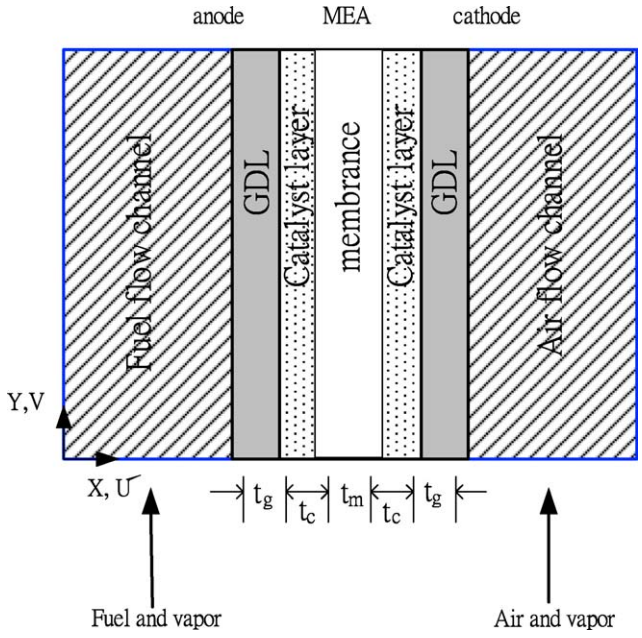

Fig. 1. Schematic diagram of a complete PEMFC and coordinate system.

simplify the problem, a steady state, 2D, multi-species, and along-the-channel model of a full-cell PEMFC is employed for the study. There are four species: hydrogen, oxygen, nitrogen, and water vapor considered in this analysis. Stationary conditions are assumed in this fuel cell, also the effect of gravity is neglected. It is assumed that the electrochemical reactions takes place only in the catalyst layer, and the gas mixtures in the flow channels are also considered to be perfect gases. Based on the definition of the Reynolds number and the velocity used in this work, the flow in the fuel cell is laminar. Therefore, all the transport equations were formulated for laminar behavior. The GDL, catalyst layer and PEM are assumed to be isotropically porous materials.

According to the descriptions and assumption above, the basic transport equations for the 2D PEM fuel cell are given as the following:

- Continuity equation:

$$\frac{\partial U}{\partial X} + \frac{\partial V}{\partial Y} = 0 \tag{1}$$

- Momentum equation:

$$U\frac{\partial U}{\partial X} + V\frac{\partial U}{\partial Y} = -\frac{1}{\rho}\frac{\partial P}{\partial X} + \nu\left(\frac{\partial^2 U}{\partial X^2} + \frac{\partial^2 U}{\partial Y^2}\right) + S_x \tag{2}$$

$$U\frac{\partial V}{\partial X} + V\frac{\partial V}{\partial Y} = -\frac{1}{\rho}\frac{\partial P}{\partial Y} + \nu\left(\frac{\partial^2 V}{\partial X^2} + \frac{\partial^2 V}{\partial Y^2}\right) + S_y \tag{3}$$

- Species equation:

$$\varepsilon_{k,\mathrm{eff}}\left(U\frac{\partial C_i}{\partial X} + V\frac{\partial C_i}{\partial Y}\right) = D_{i,\mathrm{eff}}\left(\frac{\partial^2 C_i}{\partial X^2} + \frac{\partial^2 C_i}{\partial Y^2}\right) + S_c + S_L \tag{4}$$

In the momentum equations, S_x and S_y stand for the source terms based on the Darcy's drag forces in the X and Y directions imposed by the pore walls on the fluid, and usually cause in a significant pressure drop across the porous media. The details of S_x and S_y for different layers are listed in Table 1. In Table 1, the $\varepsilon_{k,\mathrm{eff}}$ is the effective porosity, τ the tortuosity of the pores in porous medium, C_F represents the quadratic drag factor, k the permeability for the porous medium, Z_f the charge transfer coefficient, C_{H^+} is the concentration of proton, F is the Faraday constant and Φ represents the membrane potential. In the analysis, Blake–Kozeny equation [31] is used to model k as below:

$$k = \left(\frac{D_{IP}^2}{150}\right)\left[\frac{\varepsilon_{k,\mathrm{eff}}^3}{(1-\varepsilon_{k,\mathrm{eff}})^2}\right] \tag{5}$$

where $D_{IP} = 6R_{VS}$, and R_{VS} is the volume-to-surface ratio of the porous material. The parameters j_a and j_c in Table 1 indicate the current density at the anode and cathode sides, respectively, and can be described by the following Butler–Volmer equations:

$$j_a = Aj_0^{\mathrm{ref}}\left(\frac{C_{H_2}}{C_{H_2}^{\mathrm{ref}}}\right)^{1/2}\left[e^{(\alpha_a F/RT)\eta} - \frac{1}{e^{(\alpha_c F/RT)\eta}}\right] \tag{6}$$

$$j_c = Aj_0^{\mathrm{ref}}\left(\frac{C_{O_2}}{C_{O_2}^{\mathrm{ref}}}\right)\left[e^{(\alpha_a F/RT)\eta} - \frac{1}{e^{(\alpha_c F/RT)\eta}}\right] \tag{7}$$

where Aj_0^{ref} is the exchange current density, α_a and α_c the electric charge transport rates in anode and cathode catalyst layers, η the over-potential, R the gas constant and T is the temperature of the fuel cell.

Table 1
Detailed expressions of the source terms in the governing equations

	S_x	S_y	S_c	$D_{i,\mathrm{eff}}$	τ
Gas diffuser layer	$-\frac{\nu\varepsilon_{g,\mathrm{eff}}}{k}U - \frac{\varepsilon_{g,\mathrm{eff}}^2 C_F\rho U}{\sqrt{k}}\sqrt{U^2+V^2}$	$-\frac{\nu\varepsilon_{g,\mathrm{eff}}}{k}V - \frac{\varepsilon_{g,\mathrm{eff}}^2 C_F\rho V}{\sqrt{k}}\sqrt{U^2+V^2}$	0	$D_i\cdot\varepsilon_{g,\mathrm{eff}}^{\tau}$	1.5
Catalyst layer	$-\frac{\nu\varepsilon_{c,\mathrm{eff}}}{k}U - \frac{\varepsilon_{c,\mathrm{eff}}^2 C_F\rho U}{\sqrt{k}}\sqrt{U^2+V^2}$	$-\frac{\nu\varepsilon_{c,\mathrm{eff}}}{k}V - \frac{\varepsilon_{c,\mathrm{eff}}^2 C_F\rho V}{\sqrt{k}}\sqrt{U^2+V^2}$	H_2: $-(1/2FC_a)j_a$; O_2: $-(1/4FC_c)j_c$; H_2O: $(1/2FC_c)j_c$	$D_i\cdot\varepsilon_{c,\mathrm{eff}}^{\tau}$	1.5
PEM	$-\frac{\nu\varepsilon_{m,\mathrm{eff}}^2}{k}U - \frac{\varepsilon_{m,\mathrm{eff}}^3 C_F\rho U}{\sqrt{k}}\sqrt{U^2+V^2} + \frac{k}{\nu}Z_f C_{H^+}F\cdot\nabla\Phi\cdot\frac{\partial U}{\partial X}$	$-\frac{\nu\varepsilon_{m,\mathrm{eff}}^2}{k}V - \frac{\varepsilon_{m,\mathrm{eff}}^3 C_F\rho V}{\sqrt{k}}\sqrt{U^2+V^2} + \frac{k}{\nu}Z_f C_{H^+}F\cdot\nabla\Phi\cdot\frac{\partial V}{\partial Y}$	$\frac{ZF}{RT}D_{i,\mathrm{eff},H^+}C_{H^+}\left(\frac{\partial^2\Phi}{\partial X^2} + \frac{\partial^2\Phi}{\partial Y^2}\right)$	$D_i\cdot\varepsilon_{m,\mathrm{eff}}^{\tau}$	6

In Eq. (4), S_c is the production rates of i-th species in gas phase, and $D_{i,\text{eff}}$ is the effective mass diffusivity, and S_L represents the quality of liquid water in order to investigate the liquid water effect in this work. The model modifies the mass diffusivity due to the liquid water filling the pores in the porous media and the liquid generation in the species equation. When the partial pressure of water vapor is greater than the saturation pressure of water vapor, the water vapor is assumed to condense and fill the pore in the porous media. Therefore, S_L can be evaluated by the following [6]:

$$S_L = \begin{cases} M_{H_2O} k_c (\varepsilon_{\text{eff}} C_{H_2O}/\rho RT)(P_{H_2O} - P_{\text{sat}}), & \text{if } P_{H_2O} > P_{\text{sat}} \\ k_e \varepsilon_{\text{eff}} s (P_{\text{sat}} - P_{H_2O}), & \text{if } P_{H_2O} < P_{\text{sat}} \end{cases} \quad (8)$$

where the M is the molecular weight and k_c and k_e are the condensation and evaporation rate constants, respectively. The saturation pressure of water can be expressed as [13]

$$P_{\text{sat}} = 10^{-2.1794+0.02953T-9.1837\times10^{-5}T^2+1.4454\times10^{-7}T^3} \quad (9)$$

In addition, the saturation, s, is defined as the ratio of the volume of pore occupied by liquid water to the volume of pore in the porous medium, then the effective porosity of porous media is modified to account the liquid water effect,

$$\varepsilon_{\text{eff}} = \varepsilon(1 - s) \quad (10)$$

In order to evaluate the distributions of the local current density, the phase potential equation should be solved,

$$\frac{\partial}{\partial X}\left(\sigma_m \frac{\partial \Phi}{\partial X}\right) + \frac{\partial}{\partial Y}\left(\sigma_m \frac{\partial \Phi}{\partial Y}\right) = S_j \quad (11)$$

where S_j is $-j_a$ in the anode, $-j_c$ in the cathode and 0 in the membrane; σ_m is the electric conductivity of the membrane which can be calculated by the equation developed by Springer et al. [13]:

$$\sigma_m(T) = \sigma_m^{\text{ref}} \exp\left[1268\left(\frac{1}{303} - \frac{1}{T}\right)\right] \quad (12)$$

and the reference electric conductivity is

$$\sigma_m^{\text{ref}} = 0.005139\lambda - 0.00326 \quad (13)$$

$$\lambda = \begin{cases} 0.043 + 17.81a - 39.85a^2 + 36.0a^3 & 0 \le a \le 1 \\ 14 + 1.4(a-1) & 1 < a \le 3 \end{cases} \quad (14)$$

where a is the activity of water vapor at the cathode side. Using the following relations between the phase potential Φ and current density i:

$$i_x = -\sigma_m \frac{\partial \Phi}{\partial X} \quad (15)$$

$$i_y = -\sigma_m \frac{\partial \Phi}{\partial Y} \quad (16)$$

Therefore, Eq. (11) can then be reduced to be

$$\frac{\partial i_x}{\partial X} + \frac{\partial i_y}{\partial Y} = j_a \quad \text{at anode} \quad (17)$$

$$\frac{\partial i_x}{\partial X} + \frac{\partial i_y}{\partial Y} = j_c \quad \text{at cathode} \quad (18)$$

Boundary conditions for the dependent variables of the transport equations at the interfaces between different layers of the same domain are not required. A fully developed flow condition is assumed at the channel outlet, therefore,

$$U = \frac{\partial V}{\partial Y} = \frac{\partial C_i}{\partial Y} = 0 \quad (19)$$

The boundary conditions at the gas flow channel walls are

$$U = V = \frac{\partial C_i}{\partial X} = 0 \quad (20)$$

In practical situations, the physical properties, such as velocity and concentration, and their gradients are continuous on the interface. So the natural boundary conditions on the interface are the same velocity, same concentration and the same gradients of both velocity and concentration. At the interfaces between the gas diffusers and the gas channels, the following boundary conditions are used,

$$\varepsilon_{\text{eff},X^+} \left.\frac{\partial V}{\partial X}\right|_{X=X^+} = \left.\frac{\partial V}{\partial X}\right|_{X=X^-}, \quad V_{X=X^+} = V_{X=X^-} \quad (21)$$

$$\varepsilon_{\text{eff},X^+} \left.\frac{\partial C_i}{\partial X}\right|_{X=X_1^+} = \left.\frac{\partial C_i}{\partial X}\right|_{X=X_1^-}, \quad C_{i,X=X^+} = C_{i,X=X^-} \quad (22)$$

Similar conditions are employed for the interfaces between the gas diffuser layer and the catalyst layers and the interfaces between the catalyst layers and membrane can be expressed as follows:

$$\varepsilon_{\text{eff},X^+} \left.\frac{\partial V}{\partial X}\right|_{X=X^+} = \varepsilon_{\text{eff},X^-} \left.\frac{\partial V}{\partial X}\right|_{X=X^-}, \quad V_{X=X^+} = V_{X=X^-} \quad (23)$$

$$\varepsilon_{\text{eff},X^+} \left.\frac{\partial C_i}{\partial X}\right|_{X=X^+} = \varepsilon_{\text{eff},X^-} \left.\frac{\partial C_i}{\partial X}\right|_{X=X^-}, \quad C_{i,X=X^+} = C_{i,X=X^-} \quad (24)$$

The boundary conditions for the phase potential at the interface between the catalyst layer and the membrane are $\Phi = 0$ at the anode side, and $\partial\Phi/\partial X = 0$ at the cathode side. Because the phase potential is a linear distribution in the membrane, the phase potential boundary condition can be written as $\partial\Phi/\partial Y = 0$.

3. Numerical method

The solution to the governing equations is performed using a finite volume scheme by dividing the model domain into a number of cells as control volumes. In the finite volume method, the governing equations are numerically integrated over each of these computational cells or control volumes. The finite volume method exploits a collocated cell-centered variable arrangement, that implies all the dependent variables and material properties are stored at the cell center. The average value of any quantity within a control volume is given by its value at the cell center.

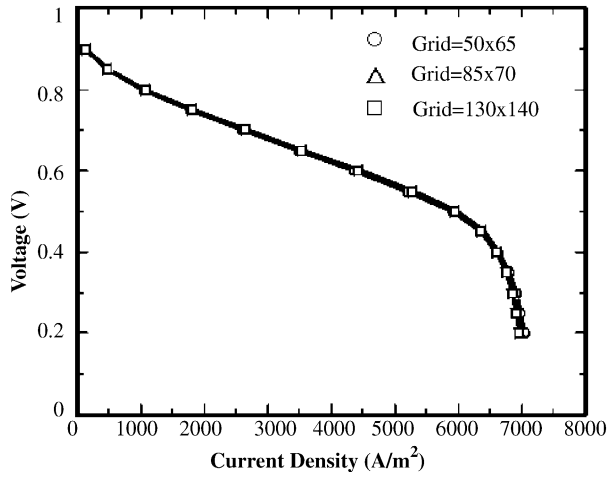

Fig. 2. Comparison of predictions for various grid systems.

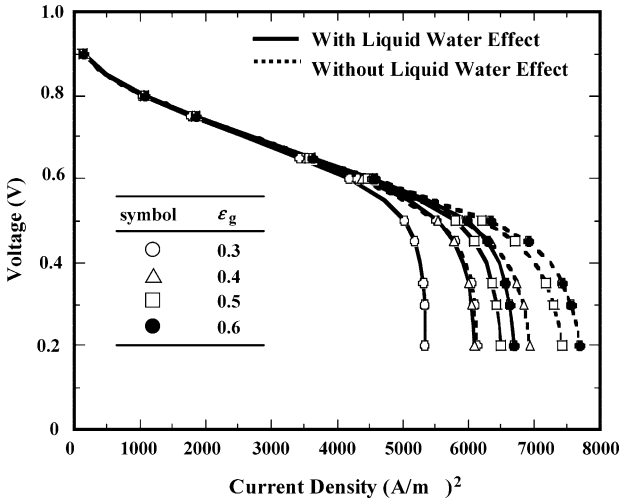

Fig. 3. Effects of the GDL porosity on the polarization curves of the PEMFC with/without liquid water effects.

The governing equations can be expressed in the form of a generalized transport equation:

$$\nabla \cdot (\rho \vec{u}\phi - \Gamma_\phi \nabla \phi) = S_\phi \tag{25}$$

where ϕ denotes the general dependent variable, Γ_ϕ the exchange coefficient, S_ϕ the source term, $\vec{u}$ represents the velocity vector, and ρ is the density. With the discretization of the governing equations, the coupled finite-difference equations can be expressed in the form of

$$a_P\phi_P = a_E\phi_E + a_W\phi_W + a_N\phi_N + a_S\phi_S + S_\phi \tag{26}$$

where ϕ_P is the value of ϕ at the current point P, $\phi_E \ldots \phi_S$ stand for the values of the grid points adjacent to the point P, and $a_P \ldots a_s$ are known as the link coefficients.

In this work, the non-uniform grid system of 85×70 is employed for the analysis. In order to examine the grid independence of the predictions, coarse and fine grid systems are considered in the preliminary tests. Effects of the grid number on the predictions of local current density are shown in Fig. 2. The maximum deviations among the computations on the grids of 50×35, 85×70 and 130×140 are less than 3%. Therefore, the grid system of 85×70 points seems to be sufficient to resolve the behaviors of the reactant gas transport in the present PEMFC model.

4. Results and discussions

The inlet conditions for the PEM fuel cell are the inlet pressure with 101.3 kPa, inlet temperature with 333.15 K, relative humidity with 100% and inlet velocity with 1 m s^{-1} for both anode and cathode. The total length of the flow channel is 14 cm, and the cross-section of the flow channel is 1 mm × 1 mm. The thicknesses of the catalyst layer and the membrane are fixed and taken to be 0.0000287 and 0.00175 m, respectively. In this study, the effects of the GDL porosity ranging from 0.3 to 0.6 and thickness ranging from 0.0002 to 0.0006 m are examined. Results without liquid water are also investigated as well as the flow direction effect.

Fig. 3 shows the polarization (*I–V*) curves with various GDL porosity of a fuel cell to investigate the influence of GDL porosity on the cell performance. The results without liquid water effects are also presented for comparison. It shows in Fig. 3 that the effect of the GDL porosity on the cell performance is significant at low operating conditions. However, at high operating conditions, the influence of GDL porosity on the *I–V* curve is negligibly small. It is also observed that the cell performance is increased as the GDL porosity increases with/without consideration of liquid water effect. For a GDL with higher porosity contains much void, which allows more gas reactant transfer into catalyst layer, in turns, more chemical reaction occurs and resulted in a better cell performance. In addition, it is noticed that the *I–V* curve is over-predicted when the liquid water effect is not taken into account in the modeling. This can be explained by the fact that the void in the GDL is filled with the liquid water, which in turn, causes the reduction of mass transfer. It is also found in Fig. 3 that the cell performance differences between the results with and without consideration of liquid water effects are small at high operating voltage conditions. It means that the fuel transport in the PEMFC can be treated as single gas phase at high voltage conditions. However, the liquid water effects on the cell performance are remarkable and cannot be neglected in the modeling at low voltage conditions. This confirms the fact that the mass transports are significant at lower voltage operating conditions and, in turn, more water is generated in the catalyst layer of the cathode side. Therefore, two-phase flow effects should be considered under low operating voltage conditions.

It is important in the design of a PEM fuel cell to realize the distribution of the fuel gases in the catalyst layer. The hydrogen mass flux distributions in the catalyst layer at the operating voltage of 0.2 V with liquid water effect are shown in Fig. 4 for the GDL porosity is 0.3, 0.4, 0.5 and 0.6. The interface of catalyst layer and membrane is on the right side, while the interface of the GDL and the catalyst layer is on the left. It is seen that the mass flux of hydrogen decreases along the axial direction due to the reaction of the hydrogen. Besides, the hydrogen

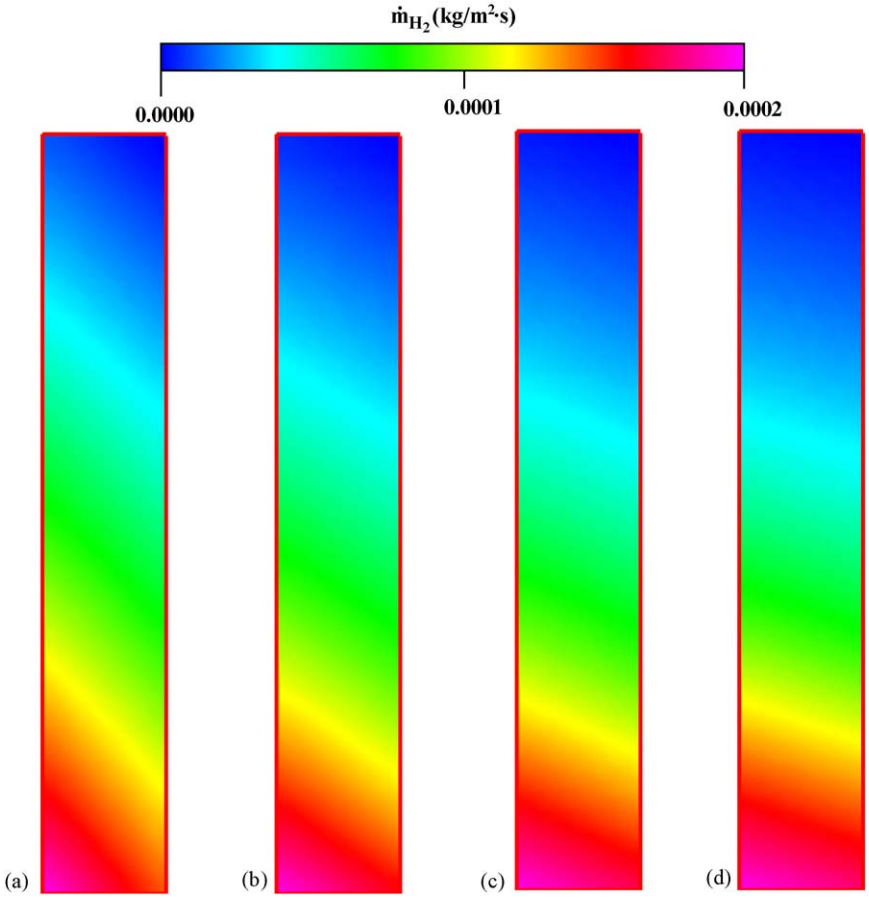

Fig. 4. Effects of the GDL porosity on the fuel mass flux in the anode catalyst layer: (a) $\varepsilon_g = 0.3$; (b) $\varepsilon_g = 0.4$; (c) $\varepsilon_g = 0.5$; (d) $\varepsilon_g = 0.6$.

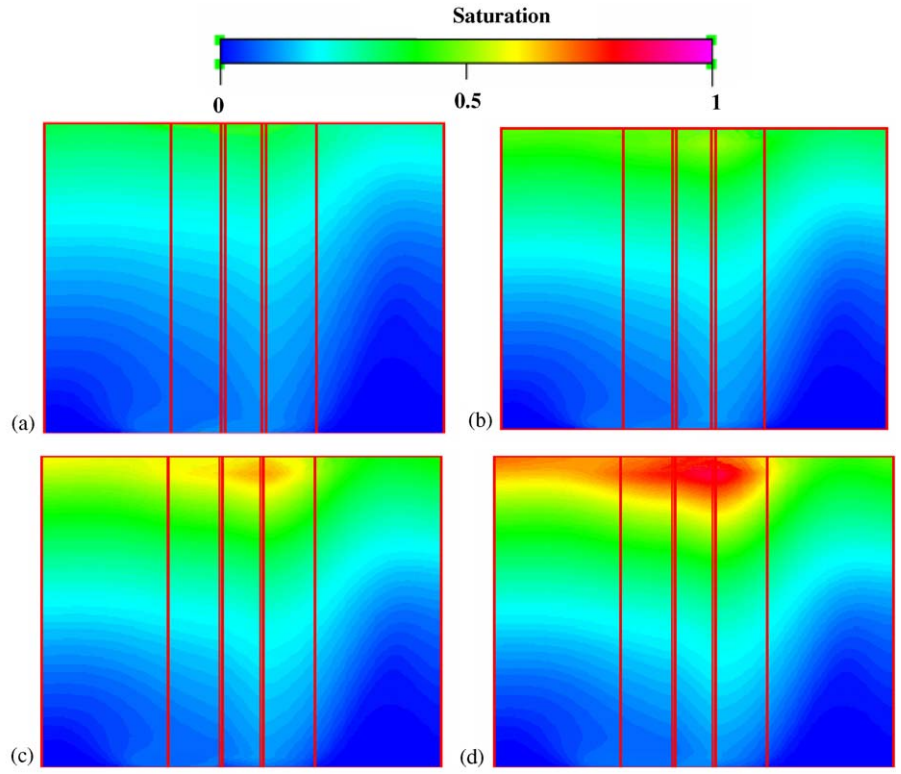

Fig. 5. Effect of the GDL porosity on the liquid water distribution for a full-cell PEMFC: (a) $\varepsilon_g = 0.3$; (b) $\varepsilon_g = 0.4$; (c) $\varepsilon_g = 0.5$; (d) $\varepsilon_g = 0.6$.

mass flux decreases along the *X*-direction. Results show that the mass flux of the hydrogen decreases as the porosity increases. This means that the consumption of the fuel gases increases as the GDL porosity increases. This again confirms the result mentioned above. The liquid water saturation distribution at the operating voltage of 0.2 V for the whole fuel cell is shown in Fig. 5 with different GDL porosities. As saturation equals to 0 indicates that there is no liquid water produced, while saturation equals to 1 indicates that the porous material is filled fully with liquid water. An overall inspection on Fig. 5 indicates that the GDL porosity affects on the liquid water production dramatically. This may be explained by the fact that the electrochemical reaction rate is high at lower operating voltages and more mass transfer for higher GDL porosity, which can thus generate more liquid water. It is also seen that the liquid water increases along the axial location and the peak value of liquid water locates at the cathode catalyst layer. This is due to the liquid water generation occurring at the catalyst layer of the cathode side.

The effect of the GDL thickness on the *I–V* curve of a PEM fuel cell is shown in Fig. 6. It is obvious that the cell performance

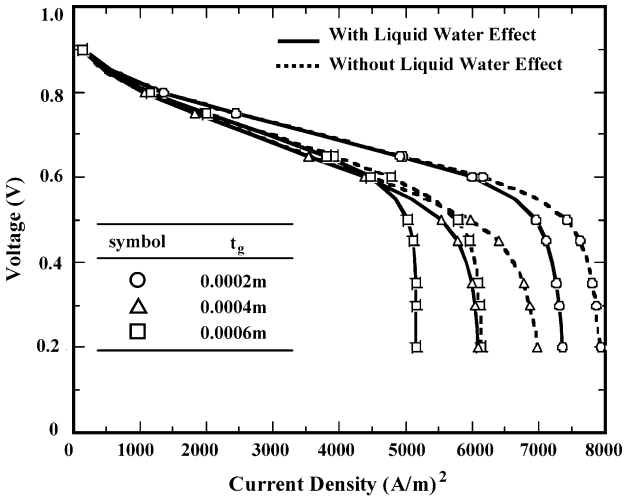

Fig. 6. Effects of the GDL thickness on the polarization curves of the PEMFC with/without liquid water effects.

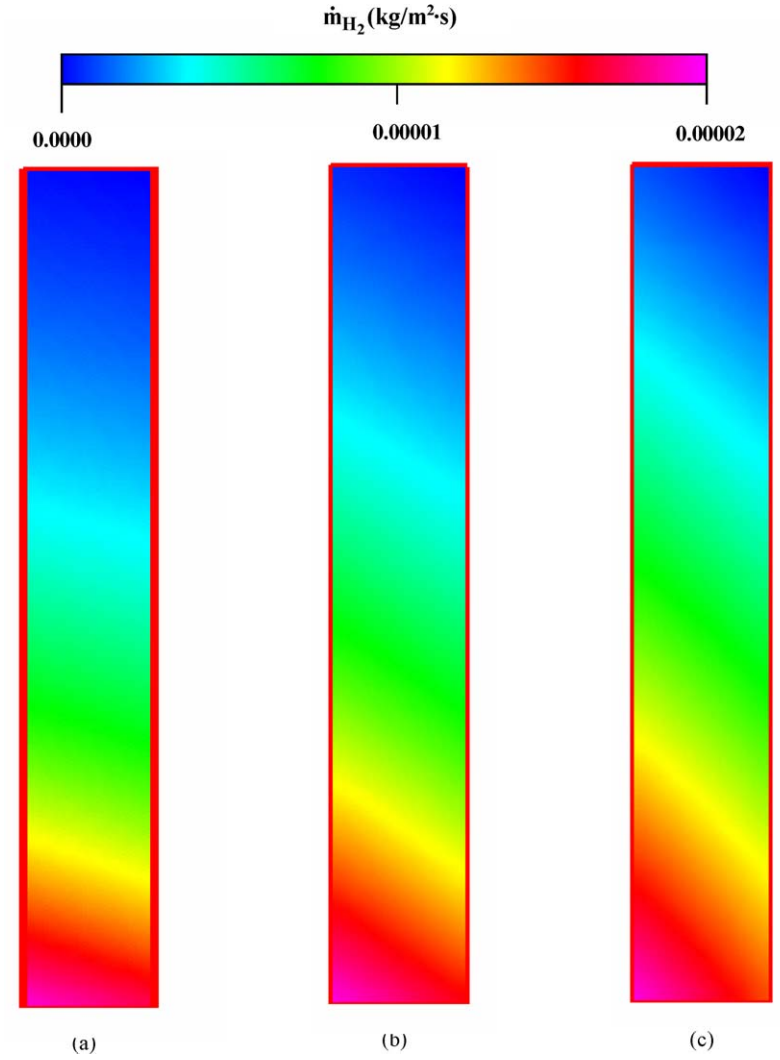

Fig. 7. Effects of the GDL thickness on the fuel mass flux in the anode catalyst layer: (a) $t_g = 0.0002$ m; (b) $t_g = 0.0004$ m; (c) $t_g = 0.0006$ m.

with or without liquid water effect increases as the GDL thickness decreases, especially at lower operating voltage conditions. For a thinner GDL, the concentration gradient becomes larger causing a higher mass transfer into the catalyst layer. Therefore, a larger current density takes place at a lower operating condition. However, it does not indicate the same trend at higher operating conditions for $V > 0.6$ V. Fig. 7 presents the hydrogen mass flux distribution in the catalyst layer with various GDL thicknesses at the operating voltage of 0.2 V. It is observed that the hydrogen mass flux increases as the GDL thickness increases.

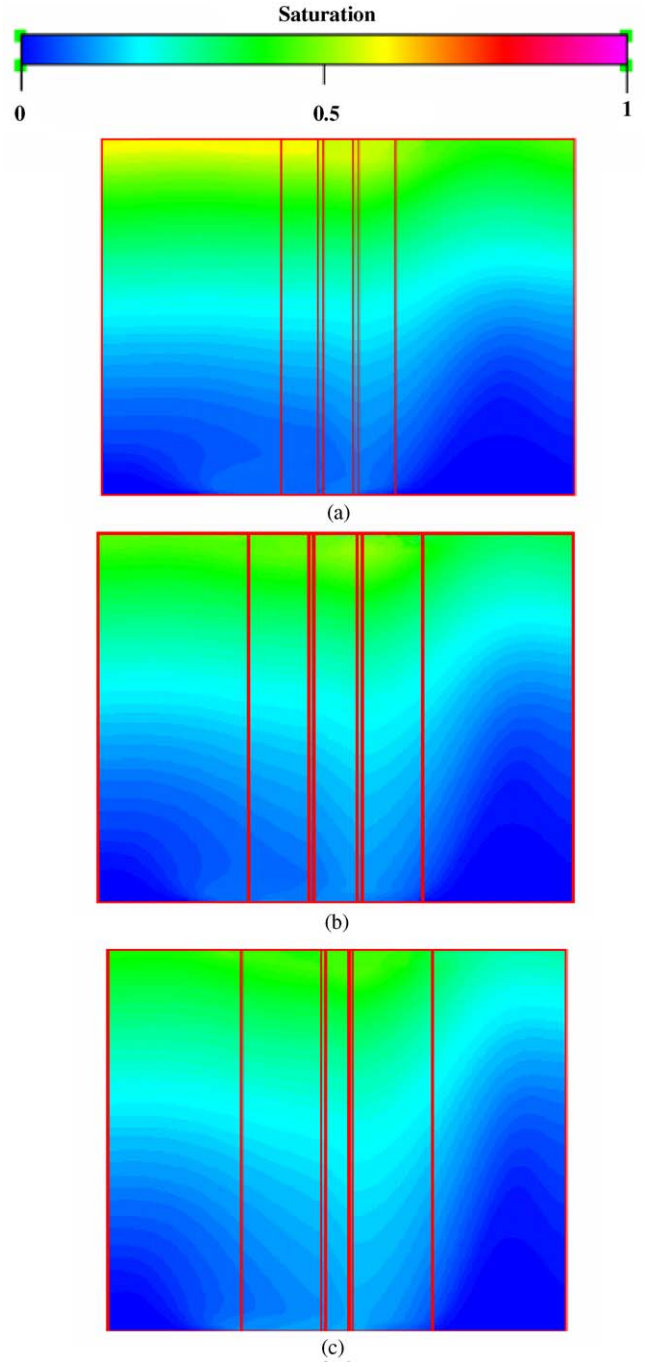

Fig. 8. Effect of the GDL thickness on the liquid water distribution for a full-cell PEMFC: (a) $t_g = 0.0002$ m; (b) $t_g = 0.0004$ m; (c) $t_g = 0.0006$ m.

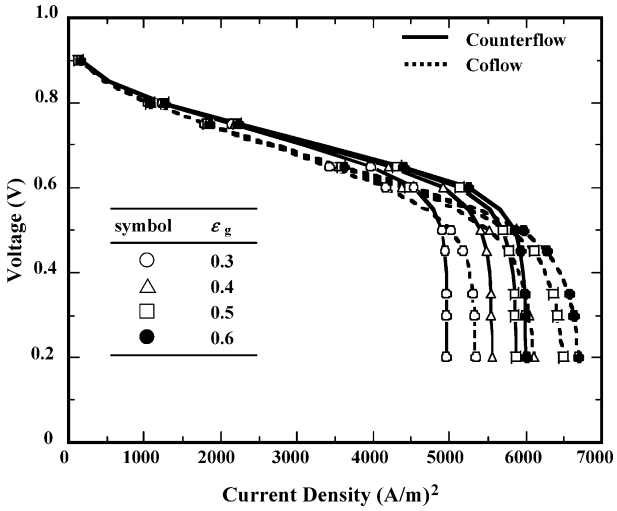

Fig. 9. Effects of the flow direction of the reactant gases on the polarization curves of the PEMFC.

This is due to the fact that the concentration gradient is smaller with a thicker GDL, which results in a smaller mass transfer of fuel gases. The liquid water saturation distributions with various GDL thicknesses for the whole cell at the operating voltage of 0.2 V are presented in Fig. 8. The saturation increases with a decrease in the GDL thickness. This is because more fuel gas transfer into the catalyst layer, which results in more liquid water generation.

The effect of the flow direction of reactant fuels in both anode and cathode on the cell performance is also studied in this work. Fig. 9 presents the effects of the GDL porosity on the cell performance with the reactant fuels in anode and cathode being co-flow and counter-flow conditions. It is found that the cell performance increases as the GDL porosity increases for both co-flow and counter-flow conditions. It is also discovered that the cell performance with counter-flow condition is better at higher operating voltage conditions, while the cell performance with co-flow condition is better at lower operating voltage conditions. Fig. 10 depicts the distributions of hydrogen mass flux in the catalyst layer with counter-flow at the operating voltage of 0.2 V. It is observed that the hydrogen mass flux decreases as the GDL porosity increases with counter-flow condition. The reason is the same as that with co-flow condition. Comparison of the corresponding results in Figs. 4 and 10 discloses that the hydrogen mass flux in counter-flow condition is lower than that in co-flow condition for various GDL porosities. This indicates that the hydrogen consumption is smaller with counter-flow condition. This is consistent to the result that the cell performance of co-flow condition is better than that of counter-flow condition at lower operating voltages. The liquid water saturation distributions at the operating voltage of 0.2 V with counter-flow condition in a full cell for various GDL porosities are shown in Fig. 11. It is found that the cathode GDL and catalyst layer are also filled with liquid water. Comparison of the corresponding curves in Figs. 5 and 11 indicates that the more liquid water is generated at the end of the cell with counter-flow condition, especially with $\varepsilon_g = 0.6$.

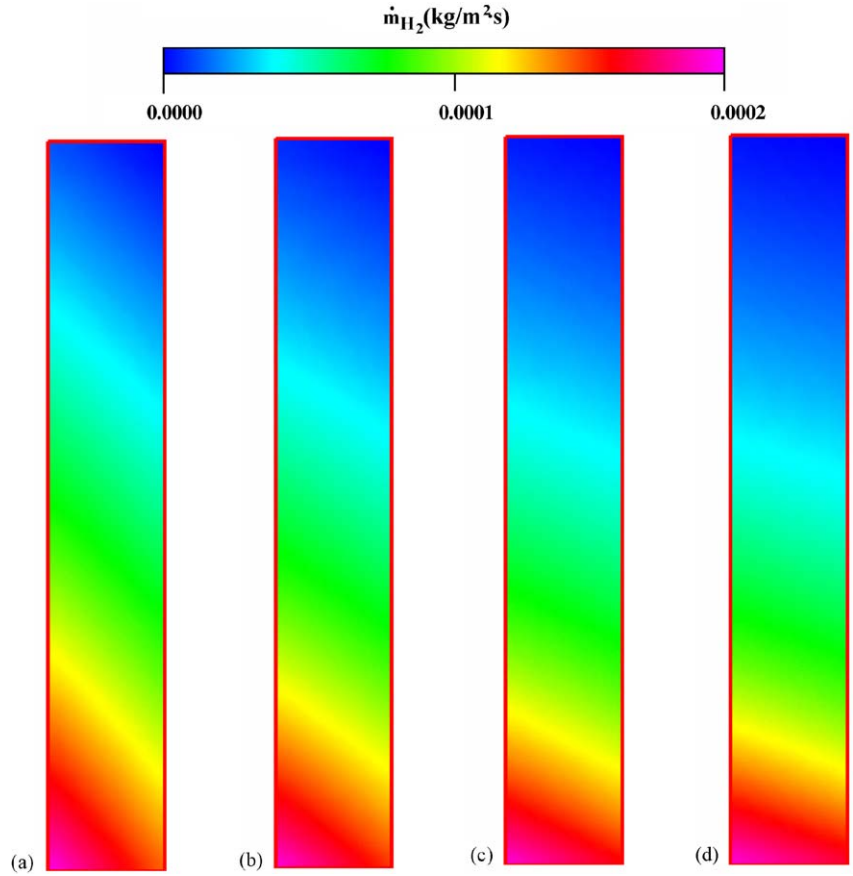

Fig. 10. Effects of the GDL porosity on the fuel mass flux in the anode catalyst layer with counterflow: (a) $\varepsilon_g = 0.3$; (b) $\varepsilon_g = 0.4$; (c) $\varepsilon_g = 0.5$; (d) $\varepsilon_g = 0.6$.

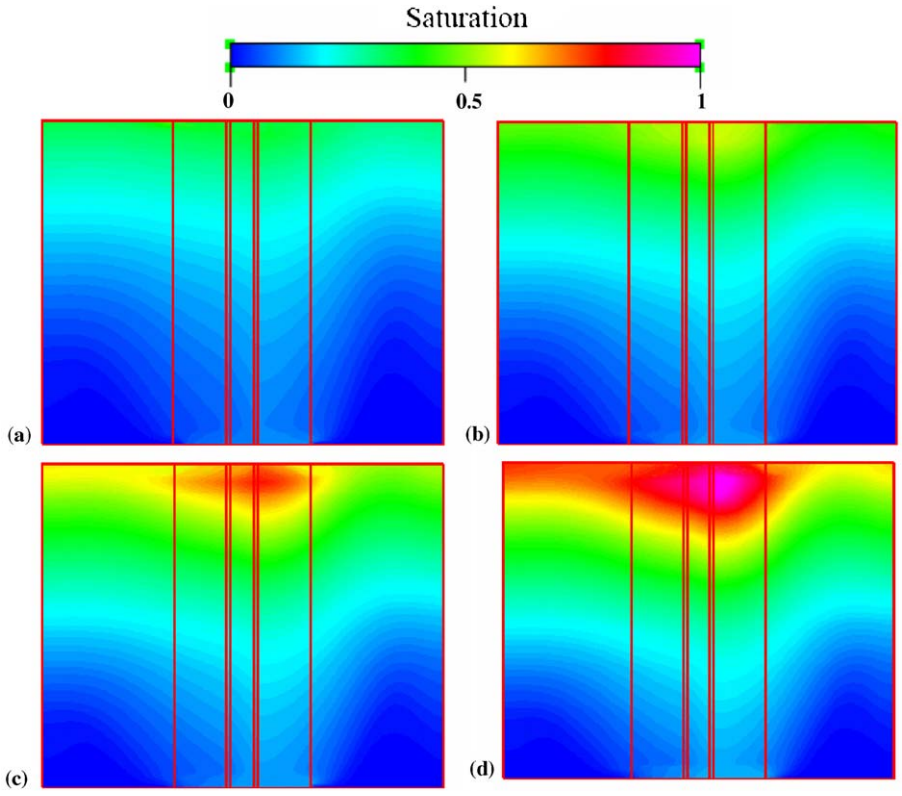

Fig. 11. Effect of the GDL porosity on the liquid water distribution for a full-cell PEMFC with counterflow: (a) $\varepsilon_g = 0.3$; (b) $\varepsilon_g = 0.4$; (c) $\varepsilon_g = 0.5$; (d) $\varepsilon_g = 0.6$.

5. Conclusion

A full-cell numerical model with steady, 2D, isothermal, multi-species has been developed to investigate the influence of the gas diffusion-layer parameters on the PEMFC. The liquid water effect is also considered in this study. The effects of the GDL porosity, the GDL thickness and the flow direction of the reactant gas on the mass transport and cell performance are examined in detail. A summary of the major results are as follows:

1. It is found that the mass transport for both the fuel and air increases as the porosity of the GDL ranging from 0.3 to 0.6 increases. Therefore, more reactant gases transfer into the catalyst layer, which in turn, leads to more chemical reaction and more reactant gases consumed. This results in a better performance for the fuel cell with a higher GDL porosity within the range of 0.3–0.6.
2. The thickness of the GDL affects the cell significantly, especially at lower operating voltages, the cell performance increases as the GDL thickness ranging from 0.0002 to 0.0006 m decreases. This is due to the fact that higher concentration gradients result from the decrease in the GDL thickness, which in turn, results in a higher mass transfer to the catalyst layer and more electrochemical reaction.
3. Liquid water effects on the cell performance are remarkable and cannot be neglected at lower operating conditions. Therefore, two-phase flow effects should be considered at low operating conditions. However, the cell performance differences between the results with and without consideration of the liquid water effects are small at higher operating voltage conditions.
4. The cell performance with the counter-flow condition is larger at the higher operating voltage conditions, while the cell performance with a co-flow condition is larger at a lower operating voltage conditions. This is due to the fact that more liquid water is generated under the counter-flow condition at lower operating voltages, and the voids in the GDL are filled with liquid water, which in turn, causes a reduction of mass transfer and a lower cell performance.

Acknowledgements

The authors would like to acknowledge the financial support of this work by the National Science Council, ROC through the contract NSC92-2212-E-211-001. The financial support from Northern Taiwan Institute of Science and Technology is also acknowledged.

References

[1] S.D. Fritts, R. Gopal, J. Electrochem. Soc. 140 (1993) 3347.
[2] A. Parthasarathy, S. Srinivasan, J. Appleby, C.R. Martin, J. Electroanal. Chem. 339 (1992) 101.
[3] R.A. Lemons, J. Power Sources 29 (1990) 251.
[4] G. Hoogers, Fuel Cell Technology Handbook, CRC Press LLC, 2002.
[5] J. Moreira, A.L. Ocampo, P.J. Sebastian, M.A. Smit, M.D. SalaZar, P. del Angel, J.A. Montoya, R. Perez, L. Martines, Int. J. Hydrogen Energy 28 (2003) 625.
[6] L.R. Jordan, A.K. Shukla, T. Behrsing, N.R. Avery, B.C. Muddle, M. Forsyth, J. Power Sources 86 (2000) 250.
[7] L.R. Jordan, A.K. Shukla, T. Behrsing, N.R. Avery, B.C. Muddle, M. Forsyth, J. Appl. Electrochem. 30 (2000) 641–646.
[8] H.K. Lee, J.H. Park, D.Y. Kim, T.H. Lee, J. Power Sources 131 (2004) 200.
[9] F. Chen, Y.Z. Wen, H.S. Chu, W.M. Yan, C.Y. Soong, J. Power Sources 128 (2004) 125.
[10] S. Mazumder, J.V. Cole, J. Electrochem. Soc. 150 (2003) A1503.
[11] S. Mazumder, J.V. Cole, J. Electrochem. Soc. 150 (2003) A1510.
[12] A.A. Kulikovsky, J. Electrochem. Soc. 150 (2003) A1432.
[13] T.E. Springer, T.A. Zawodizinski, S. Gottesfeld, J. Electrochem. Soc. 138 (1991) 2334.
[14] D.M. Bernardi, M.W. Verbrugge, AIChE J. 37 (1991) 1151.
[15] T.F. Fuller, J. Newman, J. Electrochem. Soc. 140 (1993) 1218.
[16] V. Gurau, H. Liu, S. Kakac, AIChE J. 44 (1998) 2410.
[17] I.M. Hsing, P. Futerko, Chem. Eng. Sci. 55 (2000) 4209.
[18] V. Gurau, F. Barbir, H. Liu, J. Electrochem. Soc. 147 (2000) 2468.
[19] H.S. Chu, C. Yeh, F. Chen, J. Power Sources 123 (2003) 1.
[20] W.M. Yan, C.Y. Soong, F. Chen, H.S. Chu, J. Power Sources 125 (2004) 27.
[21] A.Z. Weber, J. Newman, Chem. Rev. 104 (2004) 4679.
[22] T.V. Nguyen, R.E. White, J. Electrochem. Soc. 140 (1993) 2178.
[23] J.J. Baschuk, X. Li, J. Power Sources 86 (2000) 181.
[24] N. Djilali, D. Lu, Int. J. Therm. Sci. 41 (2002) 29.
[25] T. Berning, D.M. Lu, N. Djilali, J. Power Sources 106 (2002) 284.
[26] T.E. Springer, M.S. Wilson, S. Gottesfeld, J. Electrochem. Soc. 140 (1993) 3513.
[27] R.F. Mann, J.C. Amphlett, Mi.A.I. Hooper, H.M. Jensen, B.A. Peppley, P.R. Roberge, J. Power Sources 86 (2000) 173.
[28] Z.H. Wang, C.Y. Wang, K.S. Chen, J. Power Sources 94 (2001) 40.
[29] T. Okada, G. Xie, Y. Tanabe, J. Electroanal. Chem. 413 (1996) 49.
[30] T. Okada, G. Xie, M. Meeg, Electrochim. Acta 43 (1998) 2141.
[31] F.A.L. Dullien, Porous Media, Academic Press, New York, 1991.